

COMPARE OF DESTRUCTIVE TESTING ON NAB WELDING PROCESS

Sharda Prasad Shukla¹, Mohd Ziaulhaq²

¹M.tech Scholar, Mechanical Engineering, Azad Institute of Engineering & Technology, Lucknow, India

²Assistant Professor, Mechanical Engineering, Azad Institute of Engineering & Technology, Lucknow,

ABSTRACT-The aim of the present experimental study is to investigate the influence of the SMAW (DCEP), GTAW (DCEN) and GTAW (ACHF) process on weldability of nickel-aluminium- bronze at respective welding parameters. In this study one welding test coupon were prepared for each welding process. To accomplish this, as cast NAB welding plates P1 for SMAW, P2 for GTAW (DCEN) and P3 for GTAW (ACHF) in temper annealed condition were used Etching was then done using concentrated HNO₃ before rinsing in cold water and finally hot air drying. The specimens were then observed at a magnification of X10 and found acceptable as per ASTM rules. Transverse side bend test was then carried out to determine the weldability on test specimens measuring 155mm x 25mm x 10mm for each process. The mandrel used had a radius of 20mm; the specimen was bent to take the shape of the mandrel. The cracks so produced were observed at a magnification of X20. The method used was Vickers Hardness Test. It was found that for P1 and P2 conditions there was an increase in hardness at the weld metal and HAZ region as compared to the base metal. But for P3 condition, close readings with less hardness was seen in weld metal and HAZ region as compared to P1 and P2 condition. P2 was found to be harder. Microstructure examination was also carried out on passed weldability sample in P3 condition

keywords: Travel Speed, Heat input, hardness, macro and micro structure, bend test, SMAW, GTAW and GTAW, ACHF

INTRODUCTION

1.1- Weldability of NAB

NAB is a copper alloy having melting point around 1054°C, heat capacity 0.104 cal/g.°C and thermal conductivity 0.144 cal/cm.s.°C which is greater than three times of stainless steel. Because of high thermal conductivity, heat from weld pool sinks very quickly and may cause lack of fusion when welded with improper travel speed and heat input. Meanwhile, the characteristic that gives the alloy its corrosion resistance is the strong tenacious aluminium oxide film that forms on the surface. This causes problems of oxide film entrapment and lack of fusion during welding and must be removed.

Scraping and wire brushing the surfaces before welding is necessary.

With respect to the welding processes, TIG welding is preferred. With MIG there is no problem in dispersing the oxide film, the DC+ve current breaking up and dispersing the film. DC-ve TIG welding does not provide this cleaning action and it is necessary to use AC-TIG. Inverter-based square wave TIG power sources will give the best control. Argon is the recommended shield gas although a helium/argon mixture may be useful when welding very thick section joints with the MIG process. MMAW is possible although the fluxes required to remove the oxide film are very aggressive and may cause corrosion problems if not completely removed before the item enters service. Post weld heat treatment is rarely necessary but can be of benefit if the welded item is to experience very corrosive conditions.

The alpha phase in NAB is a predominant phase. It is a copper rich phase and is least likely to corrode. The κI phase are identified as the large globular/rosettes, κII are the dendritic rosettes; both these phases have the same composition, an iron rich aluminide, Fe₃Al, and are therefore often regarded as the same phase. κIII phase are the lamellar, eutectoids in between the alpha phases and consist of a Nickel Aluminide, NiAl in lamellar nature. It is the lamellar or continuous nature of the κIII phase which gives rise to a large proportion of closely adjacent cathodic and anodic regions, resulting in a series of micro galvanic cells which accelerate corrosion in these regions. κIV phases are spec-like, scattered throughout the alpha phase with an iron aluminide composition, Fe₃Al, these do not pose many problems due to their fine, non-continuous characteristic.

By increasing the Al content of NAB alloys to 8.8 – 10 wt. % a material with increased strength, hardness and corrosion resistance can be created. The main drawback of the increase in alloying Al is a decrease in tensile elongation and increase in kappa III phase. Li et al. investigated the effect of welding parameters using GMAW process, such as current, voltage, wire-feed rate and travel speed, on the formation of the weld bead. It was found that due to the rapid cooling rate (around 1°C/s), α with a Widmanstätten morphology, as well as bainitic and

martensitic products of β phase may become apparent, which exhibit both higher strength and ductility of the material than the slowly cooled cast metal. DREA [9] agreed that, low heat input welding of NAB predominates β martensite in HAZ, which provides good strength and ductility.

In view of above, it can be said that weldability of NAB is influenced by All steps related with welding process Purpose of the weld joints and Fabrication conditions.

There are many fusion welding processes; one of the greatest difficulties for the welding engineer is to determine which process will produce acceptable properties at the lowest cost. There are no simple answers. Any change in the part geometry, material, value of the end product, or size of the production run, as well as the availability of joining equipment, can influence the choice of joining method.

SMAW and GTAW are the two versatile fusion welding process generally used by casting industries for repair welding of cast components. At present, there has not been any work reported regarding weldability of NAB which focuses on the comparative analysis of qualitative and quantitative results of SMAW (DCEP), GTAW (DCEN) and GTAW (ACHF) of NAB components. This investigation may provide a suitable production method to significantly reduce manufacturing lead times as well as overcoming common defects trapped inside cast components.

1.2- Objective of the present work

Casting defects reduces physical properties and service performance, and is a common problem in cast NAB. Fusion welding (FW) is often used to fill casting defects or otherwise repair and join these alloys, but can also induce its own defects that include porosity, slag inclusion; lack of fusion etc. The objective of this study is to determine an optimal welding process that can be implemented to repair defective Nickel Aluminum Bronze (NAB) castings without PWHT. This study will help to understand and make a comparative analysis of SMAW (DCEP), GTAW (DCEN) and GTAW (ACHF) processes.

2. LITERATURE REVIEW

2.1- Background Information of NAB.

Aluminium bronzes are copper alloys containing, amongst other additions, up to 14% by weight of aluminium. Nickel aluminium bronzes are a subset aluminium bronzes which also contain nickel and often iron and manganese. Nickel aluminium bronzes are generally stronger than other aluminium bronzes and possess a two phase (duplex) microstructure.

2.1.1-Phases in Cast NAB

NAB is thus a copper-base alloy with a composition as given in Table 2.1. Due to a nominal 9 wt. % content of Al as-cast nickel-aluminum bronze first solidifies as the BCC beta. Further cooling of this beta phase results in decomposition of the beta to produce the four distinct phases of NAB; an FCC alpha matrix and three Kappa phases, designated kappa II, kappa III, and kappa IV. A kappa I phase only forms in alloys containing more than 5 wt.

% Fe. These kappa phases have been classified according to their individual morphologies as observed through optical microscopy, as well as according to the sequence in which they form. The phases will be explained in the order in which they form from the beta phase.

Chemical composition percent by weight of typical nickel-aluminum bronze C95800 [3].

NAB C95800	Cu	Al	Fe	Mn	Ni (inc. Co)	Si	Pb
Min.	7.9	8.5	3.5	0.8	4.0	-	-
Max.	-	9.5	4.5	1.5	5.0	0.10	0.02
Nominal	8.1	9.0	4.0	1.0	5.0	-	-

a. Alpha Phase

The alpha phase represents an equilibrium solid solution or matrix with a FCC crystal structure. Alpha forms in the vicinity of 1030°C from beta as a proeutectoid and often displays as a Widmanstätten morphology at moderate rates of cooling from the beta phase, which is consistent with the casting of components such as propellers. The alpha phase can be seen in Figure 2.3.

b. Kappa II Phase

The kappa II phase is a globular, dendritic (rosette shaped) structure found in NAB alloys containing less than 5 wt. % iron and ranges in particle size from 5 to 10 micrometers. It corresponds to an iron rich Fe3Al composition. The kappa II phase forms from beta along with the alpha phase beginning at 930°C and it is located near the lamellar eutectoid region of the

and corresponding kappa II phase is represented in Figure 2.1, 2.2 and 2.3.

c. Kappa IV Phase

Kappa IV is a fine cuboidal, cruciform precipitate formed within the alpha matrix beginning 850°C. Kappa IV particles are of the same Fe3Al composition as the kappa II phase. The kappa IV phase can be seen in Figure 2.3.

d. Kappa III Phase

The kappa III phase represents a fine lamellar eutectoid with a NiAl chemical composition. Kappa III forms at 800°C and proeutectoid kappa III is globular in morphology. The kappa III phase can be seen in Figure 2.3. The casting of NAB structures may give varied microstructures within castings due to variation in local cooling rates that also give varying material properties. Overall slow cooling rates result in relatively weak as well as heterogeneous microstructures and, in addition, porosity, which further degrades material properties. These factors ultimately lead to material with lower strength and decrease its cavitations and corrosion resistances. Additionally, poor control of the composition of NAB structures leads to inconsistent microstructures.

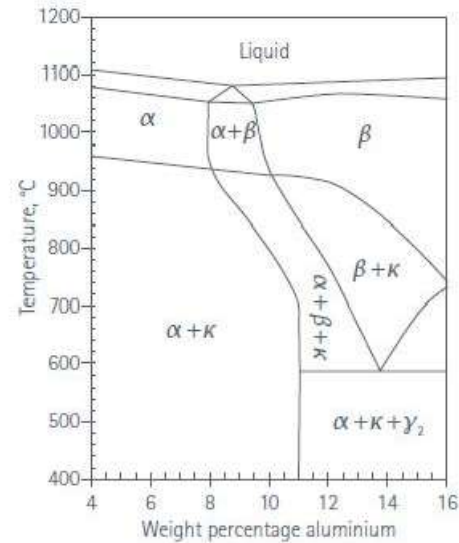


Fig2.2 Cu-Al-Ni-Fe phase diagram at 5% each of nickel and iron [10].

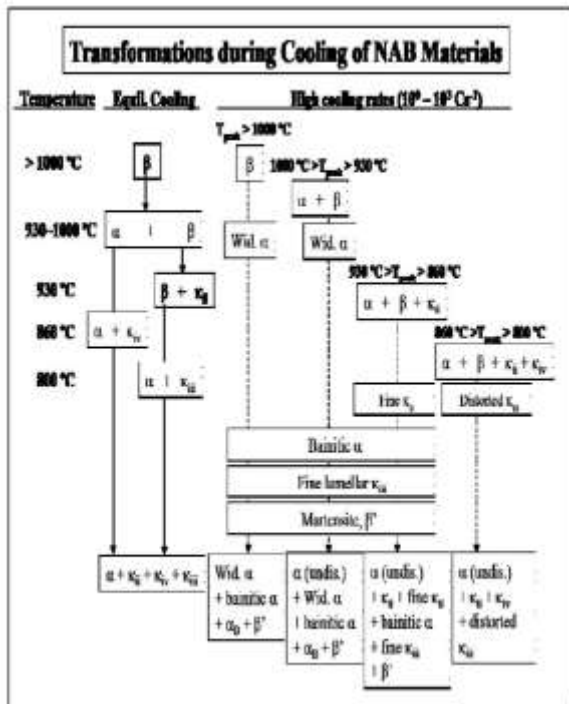


Fig2.1 Transformation of NAB Phases during Cooling of NAB Materials [1].

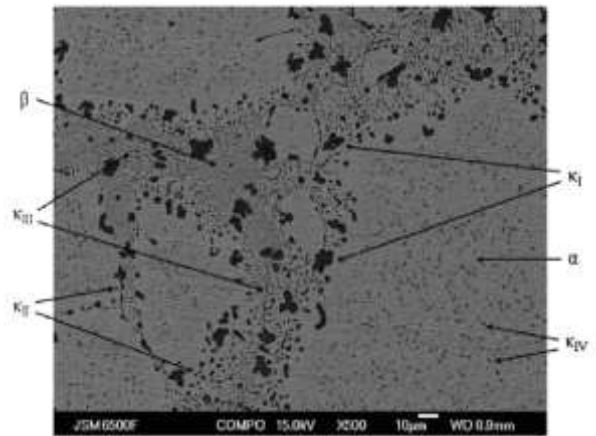


Fig2.3 Micrographic phase structure of nickel aluminium bronze - Magnification x500 [10].

2.1.2 Properties of NAB

a. Mechanical Strength: NAB's mechanical properties are better than those of Ni-Cu alloy (Monel). While there are high strength Ni-Cu wrought alloys such as K-500. Additionally, the common carbon and stainless steels materials do not differ significantly as far as these properties are concerned. The duplex and super-duplex materials are the only ones to significantly exceed the mechanical properties of NAB. Even the commonly used grades of titanium have an inferior performance to NAB.

Although the ductility of NAB is not as high as most of the materials compared, it matches titanium and, with a 15% elongation, cannot be considered brittle. The nickel

aluminium bronze offers good mechanical strength as shown in Table 2.2.

NAB C95800	
Tensile strength, minimum, ksi (MPa)	85(585)
Yield strength, E minimum, ksi (MPa)	35(240)
Elongation in 2 in. (50.8 mm), %	15
As cast or temper annealed condition.	

Table 2.2: Mechanical properties of typical nickel-aluminum bronze [3].

EXPERIMENTAL INVESTIGATIONS

3.1- Welding Set-up

The welding setup consists mainly following parts:-

a. Welding machine- This is the main part of welding setup by which controlled amount of current and voltage is supplied during welding. The inverter based Tig 4300i AC/DC (made by ESAB) is a TIG welding power source, which can also be used for MMA welding. The power welding source can be used with alternating current (AC) or direct current (DC).



Fig3.1 ESAB Tig 4300i AC/DC welding machine.

Table 3.1: Technical Specifications of Tig 4300i AC/DC

Specification	Technical details
Mains voltage	400V, ±10%, 3- 50 Hz
Voltage/current range TIG AC/DC MMA	4 - 430 A 16 - 430 A
Permissible load at TIG 40 % duty cycle 60 % duty cycle 100 % duty cycle	430 A / 27.2 V 400 A / 26.0 V 315 A / 22.6 V
Permissible load at MMA 40 % duty cycle 60 % duty cycle 100 % duty cycle	430 A / 37.2 V 400 A / 36.0 V 315 A / 32.6 V
Efficiency at maximum current TIG MMA	76 % 80 %
Open-circuit voltage TIG MMA	60 V 60 V
Cooling unit Cooling power Coolant Liquid quantity Maximum water flow	2.0 kW at 40° C temperature difference and flow 1. 0 l/min 100% water 5.5 l 2.0 l/min

b. Electrode holder, TIG welding torch and Nonconsumable tungsten electrode- For SMAW process, ESAB make 400 Amp.

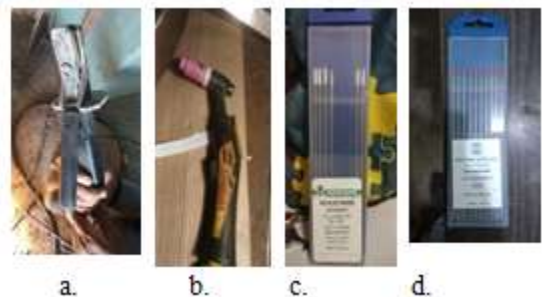


Fig3.2 a.600Amp. Handicool ESAB electrode holder. b.400 Amp. ESAB Tig welding torch. c.WOLFRAM 3.0mm Zirconiated tungsten electrode. d.WOLFRAM 3.0mm Thoriated tungsten electrode.

For GTAW process, ESAB make torch were used, Thoriated tungsten electrode for DC and Zirconiated tungsten electrode for AC as discussed in chapter 2 is fixed in the torch and Ar gas is flow through this. Electrodes and their torch are shown in figure 3.2.

c. Consumable electrode and filler wire- For SMAW process AMPCO make (SFA 5.6 ECuNiAl Ø3.2mm) consumable electrode were used. For GTAW process (SFA 5.7 ERCuNiAl Ø2.4mm) filler wire of same make were used.

d. Gas cylinder- For GTAW (AC/DC) Argon Grade 1 gas having purity level 99.99% is supplied to the welding torch with a particular flow rate so that an inert atmosphere formed and stable arc created for welding. Gas flow is control by regulator and valve

e. Work holding and clamping - A stainless steel plate is used for holding the work piece so that during welding gap between the electrode and work piece is maintained. Proper clamping using "C" clamp has been used to hold the work piece to avoid distortion.

f. Baking oven and holding oven -For SMAW process baking oven were used to preheat consumable electrode as per the recommendation of electrode manufacturer for the time specified. The baked electrodes are then transfer to holding oven at the temp.100°C

g. Digital Temperature Indicator- A calibrated EXTECH make noncontact I.R. thermometer having temperature measuring range 25°C - 800°C were used to measure interpass temperature of weld.

h. Initial and inter pass cleaning tools-It was done by chipping, SS wire brushing and deburring.



Fig.3.3 a. I.R. Thermometer. **b.** Bosch Deburring machine with point cutter. **c.** Chipping hammer. **d.** S.S. Wire brush.

3.2- Experimental planning

For the present work, experimentation was done in three processes:- In first process, partial groove welding of NAB plate P1 (25 mm thickness) done by SMAW (DCEP) process. In second process, partial groove welding of NAB plate P2 (25 mm thickness) done by GTAW (DCEN) process and In third process, partial groove welding of NAB plate P3 (25 mm thickness) done by GTAW (ACHF) process.

3.3- Experimental procedure NAB (C95800) plate as discussed in chapter 2 was selected as work piece material for the present experiment. As cast three welding plates after fettling work was machined with dimension as per ASTM A494 with the help of centre lathe, and milling done to get central groove. After that surfaces are polished with emery paper to remove any kind of external material. Plate flexible clamp side by side and welding done so that a partial groove weld can be formed for all the three processes. Before performing the actual experiment a number of trial experiments have been performed to get the appropriate parameter for each process i.e. SMAW (DCEP), GTAW (DCEN) and GTAW (ACHF)



Fig.3.4 a. Replicast NAB Test plate in Knockout area after pouring. **b.** NAB three test plate for each process after machining.

3.3.1- Process 1 (P1 SMAW-DCEP)

Stringer bead having multiple pass SMA welding with direct current electrode positive (DCEP) was used in this process. AWS/SFA A5.6 ECuNiAl of diameter 3.2 mm was taken as consumable electrode for this experiment. Test certificate is attached in Appendix-2. For the first process of experiment welding parameters selected are shown in table 3.2. Figure 3.5 shows ongoing SMAW-DCEP process.



Fig.3.5 a. Ongoing SMAW-DCEP process of NAB plate P1. **b.** NAB welded test plate P1. **c.** Welding sequence of SMAW-DCEP

Table 3.2: Welding Parameters for plate P1 SMAW-DCEP

Plate Thickness-25mm	Welding Position-PA or 1G	Welding Consumable-SFA5.6 ECUAl	Type of Joint-Partial "V" groove butt joint		
Plate drawing-As per Fig-2.6	Electrode Dia-3.2mm	Electrode Baking Temp.-300°C for 1 Hour.	Electrode Holding Temp.-100°C		
Initial and inter pass cleaning- Chipping, SS wire brushing and Deburring					
Welding Run	Current (Amp)	Voltage (V)	Travel Speed (mm/min)	Preheat/Interpass Temp.	Heat Input(kj/m m)
1.	100	23	95	44	1.1621
2.	101	23	96	46	1.1615
3.	102	23	95	45	1.1853
4.	100	23	98	58	1.1265
5.	100	23	100	52	1.1040
Average			98.48		1.1427

3.3.2-Process 2 (P2 GTAW-DCEN)

TIG welding with direct current electrode negative (DCEN) was used in these process. Thoriated tungsten electrodes of diameter 3 mm was taken as electrode for this experiment. The end of the electrode was prepared by reducing the tip diameter to 1/3 of the original diameter by grinding. For the second process of experiment welding parameters

selected are shown in table 3.3. Figure 3.6 shows ongoing GTAW-DCEN process.

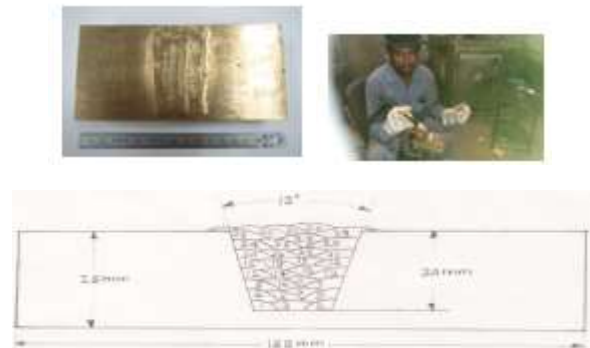


Fig.3.6 a. Ongoing GTAW-DCEN process of NAB P2 plate. **b.** NAB welded test plate P2. **c.** Welding sequence of GTAW-DCEN.

Table 3.3: Welding Parameters for plate P2 GTAW-DCEN

Thickness-25mm	Position-1G	SFA 5.4	Type of Joint-Partial "V" groove butt joint		
Plate drawing-	Ar Grade1	Size & type- EWTh-2(3.0 mm)	flow rate-08-14Ltr/min		
cup size 9.6mm	Filler 2.4mm	Initial and inter pass cleaning- SS wire brushing and Deburring			
Welding Run	Current	Voltage (V)	Travel Speed	Preheat	Heat Input kj/mm
1.	180	16	105	50	0.9874
2.	181	16	108	56	0.9653
3.	180	16	106	54	0.9781
4.	180	16	105	59	0.9874
5.	180	17	112	62	0.9836
Average			121.18		0.8679

3.3.3- Process 3 (P3 GTAW-ACHF)

TIG welding with Alternating Current High Frequency (ACHF) was used in this process. Zirconiated tungsten electrodes of diameter 3.0 mm was taken as electrode for this experiment. The ball end of the electrode was prepared by striking an arc on a scrap material piece. This creates a ball on the end of the electrode equal to its diameter. Generally an electrode that is too small for the welding current will form an excessively large ball, whereas too large an electrode will not form a satisfactory ball at all. For the third process of experiment welding

parameters selected are shown in table 3.4. Figure 3.7 shows ongoing GTAW-ACHF process



Fig.3.7 a. Ongoing GTAW-ACHF process of NAB P3 plate. b. NAB welded test plate P3. c. Welding sequence of GTAW-ACHF

Table 3.4: Welding Parameters for plate P3 GTAW-ACHF

Plate Thickness- 25mm	PA or 1G	SFA5.7 ERcCuNiAl		"V" groove butt joint	
Plate drawing	Ar Grade1	Tungsten electrode size & type-WZr8 (3mm)		Argon flow rate-10-14Ltr/min.	
Gas cup size- 11.2mm	Filler wire size 2.4mm	Initial and inter pass cleaning- SS wire brushing			
Welding Run	Current (Amp)	Voltage (V)	Travel Speed(mm/min)	PH Temp. °C	Heat Input(kj/mm)
1.	172	16	142	54	0.6977
2.	171	16	152	59	0.6480
3.	171	15	154	58	0.5996
4.	172	15	152	56	0.6111
5.	172	15	155	59	0.5992
Average Heat Input			152.58		0.6286

3.5- Test piece preparation for destructive test

After non-destructive testing was approved, all the welded plates were grinded to remove weld reinforcement and then test plates were first tack welded with dummy NAB plate for proper clamping and then cut with cutoff machine to proper strip. Two bend test specimens were machined

to proper dimension according to ASTM A494 and ASTM A488 with one extra specimen for macro and hardness test from rest of the plate.



Fig.3.8 Test sample location and cutting

3.6.2- Bend Test

Before performing bent test on all bend samples, a mandrell diameter of 40mm is calculated as per ASTM A488 and performed as per ASTM A494 & A488. Bend test was performed with universal tensile testing machine (FIE make.) with maximum load capacity of 40 Tonne.



Fig.3.9 Ongoing Bend Test on UTM machine.

3.7- Hardness Test.

Vickers hardness testing with Vickers Hardness Tester, Model: VM-50 was performed on all samples. Readings were taken in the parent metal, HAZ and weld bead. Readings were taken in each section as per EN 1043-1. Graphs of Vickers hardness were then plotted and the differences in values for the three Process plates were then analyzed in weld and HAZ region.

3.8- Metallography

From the P1 GTAW-ACHF welded plate, transverse specimen was sectioned and then grinded using successive grades of Silicon carbide paper (240, 320, 400 and 600) under running water. This was then followed by mechanical polishing on rotating wheels using diamond paste of 7µm, 1µm and 1/4µm successively and then subjected to NaOH electro etching. The metallographic specimens were then observed under a metallurgical microscope (Olympus, Japan, Model- GX 51, and Magnification 1000 X) in base metal, weld metal and HAZ region. The magnification used was X200 and X500.

3.9- Results and Discussion

A review of the results is shown in this chapter. Non-destructive testing results are examined before destructive testing

3.9.1- Weldability test result.

a. Macro Test

Three test piece of fine polished and etched weld cross section for each plates P1, P2 and P3 shows no evidence of crack, porosity, gas pocket, inadequate fusion or any other unacceptable surface imperfection.

b. Bend Test

No flaws occurred to any of the test specimens of plate P1 during testing and target bend angle was achieved with both test specimens. Plates P1 and P2 test specimens proved to be less ductile. Full records of the bend testing The observations were tabulated in Table 3.5.

Table 3.5: Maximum crack lengths for the bend test

Test Plate	Sample Reference	Maximum crack length(mm)	Figure.
P1	SB1	5.2	Fig 10
P2	SB1	2.7	Fig 11
P3	SB1	NO CRACK	Fig 12

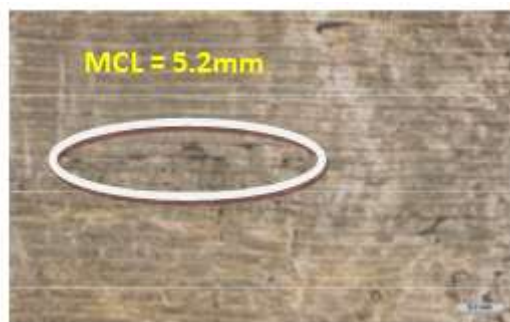


Fig.3.10 . Macroscopic image of P1 bend test specimen 1 at 20 x magnification

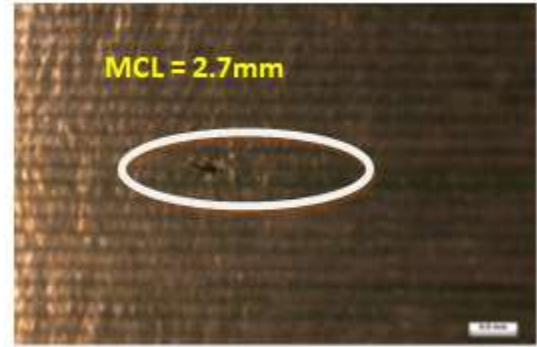


Fig.3.11 . Macroscopic image of P2 bend test specimen 1 at 20 x magnifications



Fig.3.12 Macroscopic image of P3 bend test specimen 1 at 20 x magnifications

3.9.2- Hardness Test Result

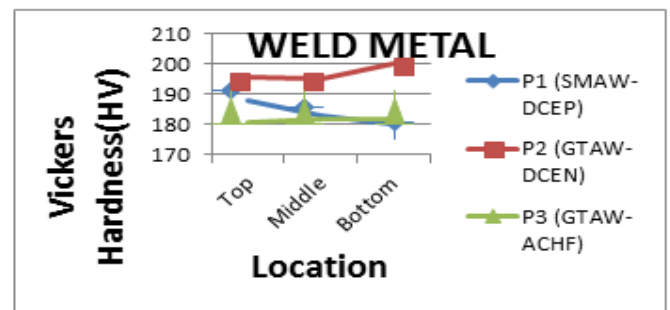


Fig.3.13 a. Comparison of Vickers Hardness value against location of multiple pass weld metal for all three welded plate condition

3.9.3- Microstructure Analysis -Two cross section specimens, 50% Base Metal 50% Weld metal and 100% Base metal, were sectioned from the welded plate (P3) sample and were prepared and etched for micro examination of weld, HAZ and base metal. The evaluations of the specimens were done using an metallurgical microscope at 200x and 500x magnification

Widmanstätten morphology

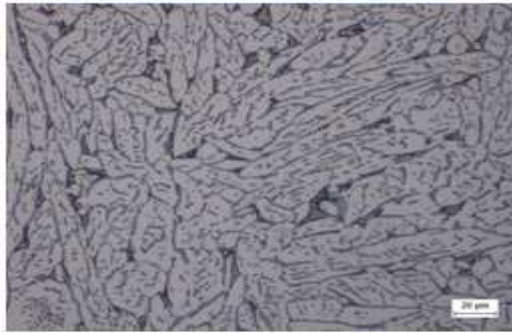


Fig.3.14. Microscopic image of weld region at 500x magnification

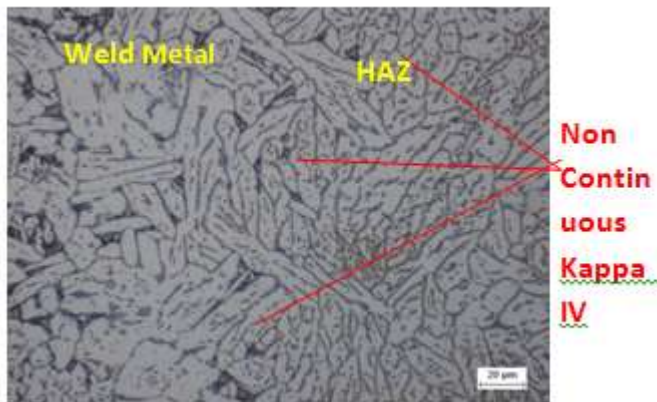


Fig.3.15. Microscopic image of HAZ region at 500x magnification

susceptibility of GTAW-ACHF is less, that will result into good weldability e. Microstructure formation in NAB during heating and cooling cycle of GTAW-ACHF process have a good control of mechanical and corrosion property in both weld metal and HAZ without PWHT

REFERENCES

- 1- ASME Sec. II B, SB148, Standard Specification for Aluminum-Bronze.
- 2-Dr. D. K. Dwivedi, Joining Technologies for Metals, IIT Roorkee, NPTEL Online Video Course , Video Lec- 9-12, 32-36,
- 3-ISO 6848, Arc Welding
- 4-Welding Handbook, Material and Applications Part 1, AWS, Eighth Edition, Vol. 3, p.163-196, 2000
- 5-ASTM, A494/A494M, Standard Specification for Castings, Nickel and Nickel Alloy, 2015
- 6.<http://www.jflf.org/v/vspfiles/assets/pdf/keyconcepts2.pdf>

4.-Conclusion

In the present work SMAW-DCEP, GTAW-DCEN and GTAW-ACHF welding processes were used to weld NAB (C95800). Following conclusions may be drawn from the study:

a. As compared to GTAW-DCEN and SMAW-DCEP processes, sound welds having higher radiography quality with less interpass cleaning effort can be achieved using GTAW-ACHF process.

b. Welding travel speeds & Heat input are key parameter of NAB welding. The joint made by GTAW-ACHF process exhibited higher travel speed and lesser heat input than GTAW-DCEN and SMAW-DCEP welding processes. GTAW-ACHF process receives a good control of mechanical properties.

d. SMAW-DCEP joint cracking susceptibility is higher as compared to GTAW-DCEN joints and highest as compared to GTAW-ACHF welded joints. As the cracking